

DTIC FILE COPY

2

TECHNICAL REPORT BRL-TR-3110

AD-A223 355

BRL

FEASIBILITY OF COSMIC-RAY MUON INTENSITY
MEASUREMENTS FOR TUNNEL DETECTION

AIVARS CELMIŅŠ

JUNE 1990

APPROVED FOR PUBLIC RELEASE; DISTRIBUTION UNLIMITED.

U.S. ARMY LABORATORY COMMAND

BALLISTIC RESEARCH LABORATORY
ABERDEEN PROVING GROUND, MARYLAND

90 06 28 024

NOTICES

Destroy this report when it is no longer needed. DO NOT return it to the originator.

Additional copies of this report may be obtained from the National Technical Information Service, U.S. Department of Commerce, 5285 Port Royal Road, Springfield, VA 22161.

The findings of this report are not to be construed as an official Department of the Army position, unless so designated by other authorized documents.

The use of trade names or manufacturers' names in this report does not constitute indorsement of any commercial product.

UNCLASSIFIED

REPORT DOCUMENTATION PAGE			Form Approved OMB No. 0704-0188	
Public reporting burden for this collection of information is estimated to average 1 hour per response, including the time for reviewing instructions, searching existing data sources, gathering and maintaining the data needed, and completing and reviewing the collection of information. Send comments regarding this burden estimate or any other aspect of this collection of information, including suggestions for reducing this burden, to Washington Headquarters Services, Directorate for Information Operations and Reports, 1215 Jefferson Davis Highway, Suite 1204, Arlington, VA 22202-4302 and to the Office of Management and Budget, Paperwork Reduction Project (0704-0188), Washington, DC 20503.				
1. AGENCY USE ONLY (Leave blank)	2. REPORT DATE JUNE 1990	3. REPORT TYPE AND DATES COVERED Final, Feb 89-Feb 90		
4. TITLE AND SUBTITLE Feasibility of Cosmic-Ray Muon Intensity Measurements for Tunnel Detection			5. FUNDING NUMBERS 612786H20001	
6. AUTHOR(S) Aivars Celmins			8. PERFORMING ORGANIZATION REPORT NUMBER	
7. PERFORMING ORGANIZATION NAME(S) AND ADDRESS(ES)				
9. SPONSORING / MONITORING AGENCY NAME(S) AND ADDRESS(ES) Ballistic Research Laboratory ATTN: SLCBR-DD-T Aberdeen Proving Ground, MD 21005-5066			10. SPONSORING / MONITORING AGENCY REPORT NUMBER BRL-TR-3110	
11. SUPPLEMENTARY NOTES				
12a. DISTRIBUTION / AVAILABILITY STATEMENT Approved for public release; distribution is unlimited.			12b. DISTRIBUTION CODE	
13. ABSTRACT (Maximum 200 words) Subsurface cosmic-ray muon intensity depends on the amount of material above the point of reference and is therefore influenced by anomalies in rock density. Because such anomalies might be caused by geological structures (e.g. ore bodies), cosmic-ray intensity measurements have been used for geophysical exploration. Recently, cosmic-ray muon intensity measurements have been also proposed as a method to detect tunnels. The feasibility of this application depends on the type of radiation detection apparatus (it must fit into a bore hole) and on the magnitude of the signal by a tunnel. If the signal is too weak, then the required observation times can become unacceptably long. In this report, the required observation times are estimated for a projected bore-hole radiation detector and for tunnels with a 2 m diameter. The estimates show that a reasonable upper bound for the detector depth is about 30 to 40 m if the observations are to be used in a tomographic reconstruction of the density field. The required observation times at that depth are of the order of days. The upper bound for the depth of detectable tunnels is less than the quoted bound for the detector depth. It might be possible to use the method at greater depths if special data interpretation techniques are developed that take into account prior knowledge about the tunnel, e.g. its anticipated direction.				
14. SUBJECT TERMS Tunnel Detection Cosmic-Ray Measurements			15. NUMBER OF PAGES 38	
17. SECURITY CLASSIFICATION OF REPORT Unclassified			16. PRICE CODE	
			18. LIMITATION OF ABSTRACT UL	
17. SECURITY CLASSIFICATION OF THIS PAGE Unclassified	18. SECURITY CLASSIFICATION OF ABSTRACT Unclassified	19. SECURITY CLASSIFICATION OF ABSTRACT Unclassified		

INTENTIONALLY LEFT BLANK.

TABLE OF CONTENTS.

	Page
LIST OF ILLUSTRATIONS	v
1. Introduction	1
2. Normal Radiation Intensity	1
3. Effect of a Tunnel on Observations with Zero Aperture	2
4. Effect of a Tunnel on Observations with Finite Aperture	4
5. Examples	6
6. Discussion of Results	7
7. Conclusions	12
LIST OF REFERENCES	14
APPENDIX. Comparison of Numerical Results	15
DISTRIBUTION LIST	31



Accession For	
NTIS COMI	<input checked="" type="checkbox"/>
DTIC TAB	<input type="checkbox"/>
Unannounced	<input type="checkbox"/>
Justification	
By	
Distribution /	
Availability Codes	
Dist. Statement /or	
Dist. Statement	
A-1	

INTENTIONALLY LEFT BLANK.

LIST OF ILLUSTRATIONS.

	Page
Figure 1. Normal radiation intensity	17
Figure 2. Tunnel coordinates	18
Figure 3. Aperture angle α	19
Figure 4. Tunnel contours and aperture field	20
Figure 5. Normal radiation intensity for a finite aperture	21
Figure 6. Normal radiation intensity in tunnel direction	22
Figure 7. Relative tunnel effect versus axial position	23
Figure 8. Absolute tunnel effect versus axial position	24
Figure 9. Relative tunnel effect in the reference plane	25
Figure 10. Absolute tunnel effect in the reference plane	26
Figure 11. Required observation effort in the reference plane	27
Figure 12. Required observation effort in the reference plane for shallow tunnels	28
Figure 13. Required observation time in the reference plane for a detector at 30 m	29
Figure 14. Required observation time in the reference plane for a detector at 40 m	30

INTENTIONALLY LEFT BLANK.

1. Introduction.

A suggestion to use underground cosmic-ray measurements for the detection of in-situ anomalies of rock density was made in 1976 by Malmquist et al. (Reference 2). The method is based on the dependency of cosmic-ray intensity on the average rock density above the detector. Because the intensity is also directional, one can determine with an appropriate detector the average rock density in a specific direction. Malmquist et al. proposed to use the method for geophysical exploration, particularly for the detection of ore bodies. Such bodies are characterized by a higher density than the surrounding rock and, therefore, cause anomalies in the observed cosmic-ray intensities at locations that are deeper than the ore. The method has also been used for the search of hidden chambers in pyramids (Alvarez et al. 1987, Reference 3). A patent for a bore-hole apparatus which measures directional cosmic-ray muon intensities has been issued in 1985 (Reference 4). The apparatus could provide a practical instrument for the detection of small anomalies, such as cavities (tunnels) in the vicinity of a bore hole. Estimates of signal strengths which can be expected from underground tunnels were presented at the Third Symposium On Tunnel Detection (Levy et al. 1988, Reference 5). In the present report we provide more elaborate estimates and discuss the feasibility of the muon radiation method for the detection of tunnels.

2. Normal Radiation Intensity.

An empirically established expression for normal muon radiation intensity in a standard Earth is (References 1 and 2)

$$I(h\rho, \theta) = I(h\rho, 0) \cdot \cos^{n(h\rho)} \theta, \quad (2.1)$$

where

$$I(h\rho, 0) = \frac{1.74 \cdot 10^6}{(400 + h\rho \cdot 10^{-3}) (11 + h\rho \cdot 10^{-3})^{1.53}} e^{-h\rho \cdot 8 \cdot 10^{-7}} \quad (2.2)$$

and

$$n(h\rho) = 1.85 + 4.65 \cdot 10^{-6} (h\rho \cdot 10^{-3})^{1.67}. \quad (2.3)$$

In these equations,

$$I = \text{muon counts} / (m^2 \cdot s \cdot \text{steradian}),$$

h = depth below the ground level (Reference 2) or below the top of the atmosphere (Reference 1), m.

ρ = average density of matter in the direction of measurement, kg/m^3 , (the average rock density at moderate depths is usually assumed to be 2700 kg/m^3).

θ = zenith angle, radians.

The formulas (2.1) and (2.2) are taken from Reference 1. They have been established from observations of radiation intensity up to depths where $h\rho = 7 \cdot 10^6 \text{ kg/m}^2$. The formula (2.3) for the exponent of the cosine is derived from a graph of the function $n(h\rho)$ in Figure 2 of Reference 1. The formula approximates the empirical curve for $h\rho \leq 2.7 \cdot 10^6 \text{ kg/m}^2$ which corresponds to about 1000 m depth. For depths less than 200 m the exponent is practically constant and equals about two.

The complicated dependence of the normal radiation on the zenith angle θ indicates that a straight ray hypothesis ("radiation intensity in a given direction is proportional to the average rock density in that direction") is only approximately true. If the hypothesis would hold exactly then at moderate depths for which the curvature of the surface of the Earth can be neglected (say, for $h < 500 \text{ m}$ or $h\rho < 1.35 \cdot 10^6 \text{ kg/m}^2$) one would have a radiation formula of the following type:

$$I(h\rho, \theta) = I\left(\frac{h\rho}{\cos \theta}, 0\right). \quad (2.4)$$

Figure 1 displays the normal radiation intensity as computed with the formulas (2.1) and (2.4), respectively. Eq. (2.1) predicts for small depths a smaller radiation intensity than the geometrical formula (2.4) whereas for large depths the trends are reversed. The reason for the difference at large depths can be the finite radius of the Earth. The reason for the difference at small depths is not clear. The crossover of the estimates occurs at about 60 metres.

For the present calculations, we shall assume eq. (2.1) as a standard and use it for nonhomogeneous rock as follows (Reference 2). First, we compute the average rock density in the direction under consideration, and then use that density and the vertical depth h in the formula. For simplicity, we shall also take the position of Reference 2 and assume that h is the depth below ground level (i.e. not below the top of the atmosphere).

3. Effect of a Tunnel on Observations with Zero Aperture.

We assume that the tunnel is an underground cavity in form of a circular cylinder with its axis parallel to the ground. Let the point of origin of a reference coordinate

system be located at the radiation detector and let the system be oriented such that the z -axis points upwards and the y -axis is parallel to the axis of the cylinder. In this coordinate system, the tunnel (the cylinder) is completely described by its radius r_0 and by the location (X_0, Z_0) of its axis in the x, z -plane (Figure 2). Let the x, z -plane be called the *reference plane*.

Let (v, ϕ, θ) be spherical coordinates related to the Cartesian coordinates of the reference system by

$$\left. \begin{aligned} x &= v \cdot \sin \theta \cdot \cos \phi , \\ y &= v \cdot \sin \theta \cdot \sin \phi , \\ z &= v \cdot \cos \theta . \end{aligned} \right\} \quad (3.1)$$

The spherical coordinates of the tunnel axis in the reference plane are

$$\left. \begin{aligned} v &= R_0 = \sqrt{X_0^2 + Z_0^2} , \\ \phi &= 0 , \\ \theta &= \Theta_0 = \arctan (X_0/Z_0) . \end{aligned} \right\} \quad (3.2)$$

The support half-angle of the tunnel cross section in the reference plane is

$$\beta_0 = \arcsin \left(r_0 / R_0 \right) . \quad (3.3)$$

The two coordinates ϕ and θ define the direction of a ray from the location of the detector. To compute the effect of the tunnel on radiation received from that direction one needs the length $D(\phi, \theta)$ of the tunnel chord along the ray. We now calculate that length.

The length of the tunnel chord along a ray $(0, \theta)$ in the reference plane is

$$D(0, \theta) = \begin{cases} 0 & \text{if } |\theta - \Theta_0| \geq \beta_0 , \\ 2 \left(r_0^2 - R_0^2 \sin^2(\theta - \Theta_0) \right)^{1/2} & \text{if } |\theta - \Theta_0| < \beta_0 . \end{cases} \quad (3.4)$$

The projection of a ray in the general direction (ϕ, θ) onto the reference plane has the slope $\cot \theta / \cos \phi$, and the zenith angle of the projection is

$$\theta_0(\phi, \theta) = \arctan \left(\cos \phi \cdot \tan \theta \right) . \quad (3.5)$$

The projection of the chord $D(\phi, \theta)$ has the length $D(0, \theta_0(\phi, \theta))$ and both lengths are related by

$$\begin{aligned}
D(\phi, \theta) &= D(0, \theta_0(\phi, \theta)) \cdot \sqrt{\sin^2 \theta_0(\phi, \theta) / \cos^2 \phi + \cos^2 \theta_0(\phi, \theta)} = \\
&= D(0, \theta_0(\phi, \theta)) / \sqrt{1 - \sin^2 \theta \sin^2 \phi} .
\end{aligned} \tag{3.6}$$

Equations (3.5) and (3.6) allow one to compute the lengths of tunnel chords along arbitrary rays from the point of origin.

Let z_{detector} be the depth of the center of origin, ρ_{rock} be the average rock density and ρ_{tunnel} be the density of matter inside the tunnel. Then the radiation intensity in the direction (ϕ, θ) is given by the normal radiation intensity formulas (2.1) through (2.3) where the argument $h\rho$ is replaced by

$$H(z_{\text{detector}}\rho_{\text{rock}}, \rho_{\text{tunnel}}, \phi, \theta) = z_{\text{detector}}\rho_{\text{rock}} + (\rho_{\text{tunnel}} - \rho_{\text{rock}}) \cdot D(\phi, \theta) \cdot \cos \theta . \tag{3.7}$$

H is a measure for the mass which shields the detector against cosmic radiation in the direction (ϕ, θ) . Obviously, if the rock is homogeneous, that is $\rho_{\text{tunnel}} = \rho_{\text{rock}}$, then $H = z_{\text{detector}}\rho_{\text{rock}}$. The absolute effect of the tunnel on the radiation intensity is the difference

$$E(z_{\text{detector}}\rho_{\text{rock}}, \rho_{\text{tunnel}}, \phi, \theta) = I(H, \theta) - I(z_{\text{detector}}\rho_{\text{rock}}, \theta) . \tag{3.8}$$

Its dimension is [counts/(m²·s·sr)]. We also define a dimensionless relative effect by

$$P(z_{\text{detector}}\rho_{\text{rock}}, \rho_{\text{tunnel}}, \phi, \theta, 0) = I(H, \theta) / I(z_{\text{detector}}\rho_{\text{rock}}, \theta) - 1 . \tag{3.9}$$

The last argument of P in eq. (3.9) is the aperture angle of the detector which is assumed to be zero in this section.

4. Effect of a Tunnel on Observations with Finite Aperture.

We define the angular aperture of the detector by specifying an aperture angle α such that the detected radiation is received from within a cone with the half-angle α (see Figure 3). The corresponding solid angle of the aperture is $2\pi(1 - \cos \alpha)$ steradians. The normal radiation which is received with the aperture α equals the integral of $I(z_{\text{detector}}\rho_{\text{rock}}, \theta)$ over all rays that are inside the aperture cone. The effect of the tunnel is obtained by comparing this integral with the integral of $I(H, \theta)$ over the same solid angle.

We need the integration limits in terms of the spherical coordinates. They are obtained by computing the intersection of the aperture cone with a sphere (with its center located at the detector) in terms of the coordinates ϕ and θ . Let the radius of the sphere be R and the axis of the cone be given by the coordinates ϕ_c and θ_c . The unit vector in the direction of the axis is

$$\vec{u}_c = \begin{pmatrix} \sin \theta_c \cdot \cos \phi_c \\ \sin \theta_c \cdot \sin \phi_c \\ \cos \theta_c \end{pmatrix} . \quad (4.1)$$

A point on the surface of the sphere is defined by the vector

$$\vec{w}(\theta, \phi) = \begin{pmatrix} R \cdot \sin \theta \cdot \cos \phi \\ R \cdot \sin \theta \cdot \sin \phi \\ R \cdot \cos \theta \end{pmatrix} . \quad (4.2)$$

Points of intersection of the sphere with the aperture cone satisfy the equation $(\vec{u}_c \cdot \vec{w}) = R \cdot \cos \alpha$ (see Figure 3). Pairs (ϕ, θ) which define rays inside the aperture cone satisfy the inequality $(\vec{u}_c \cdot \vec{w}) \geq R \cdot \cos \alpha$, or

$$C(\phi, \theta) = \sin \theta \cdot \sin \theta_c \cdot \cos(\phi - \phi_c) + \cos \theta \cdot \cos \theta_c - \cos \alpha \geq 0 . \quad (4.3)$$

The intensity of radiation observed with the aperture α in the presence of a tunnel is

$$J(z_{\text{detector}} \rho_{\text{rock}} \cdot \rho_{\text{tunnel}}, \phi_c, \theta_c, \alpha) = \int_{C(\phi, \theta) \geq 0} I(H, \theta) \cdot \sin \theta \, d\phi \, d\theta . \quad (4.4)$$

J has the dimension [muon counts/(m²·s)]. If the tunnel is not present, then an observation with the aperture α yields

$$J(z_{\text{detector}} \rho_{\text{rock}} \cdot \rho_{\text{rock}}, \phi_c, \theta_c, \alpha) = \int_{C(\phi, \theta) \geq 0} I(z_{\text{detector}} \rho_{\text{rock}}, \theta) \cdot \sin \theta \, d\phi \, d\theta . \quad (4.5)$$

The absolute effect of the tunnel is for the aperture α

$$\begin{aligned} F(z_{\text{detector}} \rho_{\text{rock}}, \rho_{\text{tunnel}}, \phi, \theta, \alpha) &= \\ &= J(z_{\text{detector}} \rho_{\text{rock}}, \rho_{\text{tunnel}}, \phi, \theta, \alpha) - J(z_{\text{detector}} \rho_{\text{rock}}, \rho_{\text{rock}}, \phi, \theta, \alpha) . \end{aligned} \quad (4.6)$$

The dimension of F is [counts/(m²·s)]. The dimensionless relative effect for a detector with the aperture α is

$$\begin{aligned} P(z_{\text{detector}} \rho_{\text{rock}}, \rho_{\text{tunnel}}, \phi, \theta, \alpha) &= \\ &= J(z_{\text{detector}} \rho_{\text{rock}}, \rho_{\text{tunnel}}, \phi, \theta, \alpha) / J(z_{\text{detector}} \rho_{\text{rock}}, \rho_{\text{rock}}, \phi, \theta, \alpha) - 1 . \end{aligned} \quad (4.7)$$

Note that the absolute effect F depends on the aperture and is proportional to α^2 if $\alpha \ll 1$. In contrast, the absolute effect E , eq. (3.8), is for a single ray and therefore does not depend on α .

5. Examples.

We illustrate the effect of a tunnel on the observed radiation intensity by calculating the radiation for a number of typical arrangements of tunnel and detector. To be specific, we assume for all calculations that the tunnel diameter is 2 m and that the detector's aperture α is 5° . The normal intensity for other small apertures can be estimated from the presented results by noting that the intensity is proportional to α^2 . A detector with a large aperture produces a stronger signal than a detector with a small aperture, but the angular resolution of the device with the smaller aperture is better. This means that the smaller the aperture the better is the accuracy with which the tunnel can be located. Figure 4 shows that an aperture of about 5° should be adequate for depth differences up to 20 m between tunnel and detector. Much larger differences of depths would require smaller apertures in order to achieve a reasonable resolution. Figure 5 displays the normal radiation intensity for a detector with an aperture of 5° . Note that the intensity in Figure 5 has a dimension different from that in Figure 1, because Figure 5 shows the integral (4.7) of the normal intensity over the aperture of the receiver, whereas Figure 1 displays the normal intensity as given by eq. (2.1). The general trends of the curves in both figures are similar.

If the aperture is finite, then the largest effect by the tunnel likely is obtained in a direction where the tunnel is closest to the detector. This direction is in the plane orthogonal to the axis of the tunnel, that is in the reference x,z -plane defined by $\phi = 0 \bmod(\pi)$. We test this property of the tunnel signature by calculating the intensity observed in directions toward points of the tunnel axis at a distance from the reference plane. Figures 6 through 8 show some of these calculations. They were made for a detector depth of 100 m, a tunnel depth of 80 m and two tunnel locations, specified by the zenith angles $\theta_0 = 0^\circ$ and 45° . In the case of zero zenith angle the tunnel is located directly above the detector at which position it has the largest effect.

Figure 6 shows the normal intensities observed in the directions of the two tunnels. The abscissa is the distance of the aim point from the reference plane. As this distance increases (we orient the detector's aperture field towards the point of the tunnel axis indicated by the abscissa) the corresponding zenith angle increases, too, and consequently the normal intensity decreases. The effect of the tunnel cannot be seen in the plotting scale of Figure 6 because the relative effect is generally less than 1% and therefore mostly within the line thickness of the curve. The relative and absolute effects of the tunnel, respectively, are shown in Figures 7 and 8. The relative increase of the intensity due to the presence of the tunnel is given by eqs. (3.9) and (4.7), and the computed results are shown in Figure 7. The dot-dash curves in the top part of Figure 7 show the relative effect of the tunnel in case of zero aperture. The two curves in the lower part of the figure show the relative effect in case of an aperture of 5° . It is interesting to note that for zero aperture the relative effect increases slightly as the axial

position increases. This is due to an increase of the tunnel chord for oblique observations. However, this effect is more than compensated by the geometrical effect of the finite aperture since the tunnel occupies a smaller part of the field of view as the distance to the tunnel increases. The absolute tunnel effect is shown in Figure 8 for the same two tunnels. The figure indicates that the effect of the tunnel decreases by a factor of ten as the distance along the tunnel axis increases to about 40 m. The axial distance of 40 m approximately corresponds in the present examples to a zenith angle of 50° .

In summary, Figures 6 through 8 confirm that the largest effect of the tunnel is indeed in the reference plane for all zenith angles of interest. Also, the effect is reduced by about a factor of ten as the zenith angle increases from zero to about 45° . Next we present some calculations of the tunnel effect in the reference plane, that is for conditions optimal for tunnel detection.

Figure 9 shows the relative effect of the tunnel in the reference plane for three different detector depths and the same two zenith angles of the tunnel as in Figures 7 and 8. If the detector is placed very close to the tunnel then the outline of the tunnel completely covers the aperture's field of view. The corresponding relative effect of the tunnel approximates the relative effect in case of zero aperture which is independent of the tunnel depth, and is shown in Figure 9 by dot-dash lines. In case of the 5° aperture, the relative effect P of the tunnel is reduced approximately by a factor of ten when the depth difference between detector and tunnel increases from zero to 50 m.

Figure 10 shows the absolute effect F of the tunnel for the same cases as shown in Figure 9. The general shape of the curves are similar to those of Figure 9 except that the rate of decrease of the absolute effect is about half of the rate of the relative effect.

6. Discussion of Results.

In the previous section we presented some examples of the effect of a tunnel on the received muon radiation intensity. The effect was found to be of the order of one percent and the accuracy of the muon counting must be much better than that if the tunnel is to be detected. The accuracy of the muon count depends on the total count and, since the total count depends on the size of the detector and duration of the observation, one can use calculations of the effect of the tunnel to find estimates of detector sizes and observation times which are necessary for a successful tunnel detection operation.

The strength of the tunnel signal is proportional to the absolute effect F , eq. (4.6), illustrated by Figure 10. In order to detect this signal it is necessary that the standard error of the observation is a fraction of the signal. We denote the fraction by ϵ and call it the *confidence factor*. Let the standard error of the muon count be σ_N , and let the

increase of the count due to the presence of the tunnel be ΔN_{tunnel} . Then the condition for the detection of the signal is

$$\sigma_N < \epsilon \cdot \Delta N_{tunnel} . \quad (6.1)$$

The signal strength is

$$\Delta N_{tunnel} = F \cdot t \cdot a , \quad (6.2)$$

where t [s] is the duration of the observation and a [m²] is the receiver area of the detector. The standard error of the count of impacting muons equals the square root of the total count, that is

$$\sigma_N = \sqrt{J \cdot t \cdot a} , \quad (6.3)$$

where J [counts/(m²·s)] is the normal radiation intensity for the given aperture, eq. (4.5). Substituting these expressions into eq. (6.1) one obtains the following condition for the product of observation time and detector area:

$$t \cdot a > \frac{1}{\epsilon^2} \frac{1}{F^2} J . \quad (6.4)$$

In terms of the relative tunnel effect P which is given by eq. (4.7) the condition for the product is

$$t \cdot a > \frac{1}{\epsilon^2} \frac{1}{J \cdot P^2} = \frac{1}{\epsilon^2} \frac{1}{F \cdot P} . \quad (6.5)$$

A reasonable value of the factor $1/\epsilon^2$ is four, corresponding to $\epsilon = 0.5$ or to a signal that is twice as large as standard error of muon counting. A more reasonable value of the factor is ten, that is $\epsilon = 0.316$ which roughly means that the signal is about three times as large as the standard error of counting. In our examples we shall use the value ten for $1/\epsilon^2$. Therefore, the estimated conditions for the product $t \cdot a$ might be relaxed possibly by a factor of two, although this is not recommended. (We have only considered the counting accuracy. Additional measurement noise can be caused by temporal and spacial variations of the muon radiation as it arrives at the Earth, and by changing conditions in the atmosphere during the recording).

The product $t \cdot a$ is a measure of the effort that is needed to produce the required result. Let it be called *observation effort*. Its dimension is s·m², which we replace by the more practical dimension days·m². Next, we compute the required observation effort for the cases shown in Figures 9 and 10.

Figure 11 shows the required observation effort for detector depths of 30, 50, 100 and 200 m. To determine whether the required effort for these cases has a manageable order of magnitude, one has to estimate the detector's receiving area a . For instance, if

the area a is about one square metre then a tunnel detection with the receiver at 100 m depth would require observations which last months or even years. To simplify the discussion we assume that the receiving area equals the silhouette of the detector, and estimate the measurements of such a device. (Actually, the effective receiving area could be a fraction of the silhouette, or a combination of several silhouettes, depending on the construction of the device and on the data recording logic).

The properties which distinguish a tunnel from geological density variations are well defined boundaries and the magnitude of the density anomaly. If the extension of the device is much larger than the tunnel diameter then the signature of the tunnel is diminished and smeared out, and it might not be possible to distinguish between geological density variations, topographic effects and the tunnel in the tomographically reconstructed density field. Therefore, we require that the linear extension of the detectors silhouette is not more than 2 m (the tunnel diameter) in a direction orthogonal to the tunnel axis. Assuming that the zenith angle of the observations is less than 45° one obtains that the vertical dimension of the detector should be less than $2/\sin 45^\circ$ or 2.82 m. The radial dimension of the detector is bounded by the diameter of the bore hole in which the detector is placed.

The detector proposed in Reference 4 has the form of a cylinder aligned with the axis of a bore hole. The device registers all those muons and the directions of their paths which penetrate the side walls of the cylinder. Thus one can assume that for vertical bore holes the apparatus will have a directional sensitivity proportional to $\sin \theta_c$, where θ_c is the zenith angle of the direction of the incoming muons. Let the length of the detector be L and its diameter be D . Then the effective recording area is approximately given by

$$a = D \cdot L \cdot \sin \theta_c \quad (6.6)$$

Following Reference 5 we assume that the bore-hole diameter is 0.30 m and the corresponding effective diameter of the detector is $D = 0.26$ m. From the resolution requirement discussed above we have $L = 2/\sin \theta_{c \max}$, where the maximum zenith angle for the observations might be about 45° . Thus, the effective recording area is given by

$$a = 0.26 \cdot \frac{2.0}{\sin \theta_{c \max}} \cdot \sin \theta_c \leq 0.52 \quad [\text{m}^2] \quad (6.7)$$

One sees from Figure 11 that with this recording area the required recording time is tens or even hundreds of days for detector depths of 50 m or more. Hence, the proposed tunnel detection method and device cannot be reasonably used for depths over 50 m.

Figure 12 shows plots of required observation effort for some detector depths less than 50 m. The plots indicate that a practical bound for detector depths is between 30 and 40 m. The required recording times at those depths are of the order of days or tens of days.

To determine the bound more accurately we assume a specific receiver area and compute the corresponding required recording times in days for detector depths of 30 m and 40 m, respectively. To compute the receiver area we use eq. (6.7) with the maximum zenith angle of 45° . (Thus, the results are for a bore-hole diameter of 30 cm and a detector length $L = 2.82$ m). Figure 13 shows the results for a 30 m detector depth and tunnel depths between 5 m and 25 m. Because we must assume that the tunnel depth is not known, the recording times have to be such that the worst case is covered. In the present example, this is the case where the tunnel is at a depth of 5 m, that is the top curve in Figure 13. (Extrapolation to a shallower tunnel at, e.g. 1.5 m should be obvious from the figure). The curve shows that one needs about ten days of observation time if the observation zenith angles are restricted to the interval between 5° and 45° . This result indicates that 30 m is a practical upper bound of the detector depth for tunnel detection operations. The corresponding maximal depth of the tunnel depends on the distance between the bore holes from which the measurements are used for the tomographic density reconstruction. In any case, the tunnel depth must be less than the depth of the detector.

To see how much the requirements change when the detector is placed at greater depths we plot in Figure 14 the required observation times for a detector depth of 40 m and tunnel depths between 5 m and 35 m. The worst case requirement (read from the 5 m curve) is now about 40 days of observation time, which seems to be too long for practical operations.

The presented estimates of required observation times depend on a number of assumptions about the mode of operation and properties of the detector. We now discuss consequences of differing assumptions about the tunnel detection method. First, a reduction of observation times by about a factor of two could be achieved by restricting the zenith angle interval of the observations because the signal of the tunnel is stronger for smaller zenith angles (see Figures 9 - 12). A consequence of such a restriction is a reduction of the explored area which means that more bore holes at closer distances would be needed to cover the same area. Second, the observation times could be reduced if the observations were made with larger apertures and longer detectors. The consequence of an increase of the aperture and detector length is a reduction of spacial resolution, that is an impairment of the detectability of the tunnel by density reconstruction. Third, the confidence factor ϵ could be increased from 0.316 to, say 0.5. As discussed above, this would decrease the required observation times by about a factor of two. Because this reduction of observation times reduces the signal to

noise ratio, it also reduces the probability of a detection of the tunnel. Finally, a small reduction of the observation time could be achieved by designing the detector such that its sensitivity is not proportional to the sine of the zenith angle thereby enhancing the sensitivity at small zenith angles. It seems, however that any combination of these modifications could possibly reduce the required observation times by not more than an order of magnitude which would increase the practical bound for the detector depth from 30 m to only about 40 m.

The conclusions in this report differ significantly from the conclusions by Levy et al. in Reference 5. Possible reasons for the differences are different formulas for the normal radiation, approximate calculations, different detector geometries, and different definitions of the effect of the tunnel. We now discuss in turn these possible sources of disagreement.

The normal radiation formula used by Levy et al. is

$$I(h\rho, \theta) = I \left(\frac{h\rho}{\cos \theta}, 0 \right) \cdot \frac{1}{\cos \theta} \quad (6.8)$$

This formula differs from the formula (2.1) used in this report and from the geometrical formula (2.4), and it is quoted by Levy et al. without derivation or reference. From Figure 1 where the geometrical formula is compared with eq. (2.1) (for $\theta = 45^\circ$) one can conclude that eq. (6.8) predicts for shallow detector depths up to three times larger radiation intensities than eq. (2.1). However, the difference between the formulas is insignificant for a detector at 100 to 200 m depth which is the principal range of interest in Reference 5.

To simplify our calculations we assumed that the detector length is small compared with the distance to the tunnel. Levy et al. do not make that assumption but do make a number of other simplifying assumptions. The precise effect of these assumptions is difficult to assess and a direct comparison of the numerical results is not possible because of differing assumptions about the detector size and definitions of the tunnel effect. An order of magnitude comparison is, however, possible and it is shown in the Appendix that results in both papers agree. Hence one might conclude that the various simplifying assumptions in both papers have not distorted the results.

We assumed in this paper that the vertical length of the detector is 2.82 m and that the radiation is recorded with a 5° aperture. We then calculated the radiation within the corresponding solid angle with and without the tunnel, and defined the tunnel effect as the difference between both computations. (The calculations were done in the reference plane, that is for the azimuth where the tunnel has the largest effect). Levy et al. assume that the detector extends from the ground surface to 200 m depth. Instead of defining an aperture cone they estimate the solid angle which is supported by the tunnel

(shown as a horizontally hatched area in Figure 4), calculate the radiation within this angle with and without the tunnel, and define the tunnel effect as the difference between these two calculations. Because of this definition, their relative as well as absolute tunnel effects are much larger than ours and, consequently, their estimates of required observation times are much shorter.

It is not obvious how the calculations by Levy et al. are related to measurements which are needed for a tomographic density reconstruction. In general, one needs for such a reconstruction the angular dependence of the signal, and observations from a number of receivers at different locations. These requirements dictated our choice of 5° for the aperture in order to register the angular dependence of the signal, and 2.82 m for the detector length in order to have a well defined detector location. (See the beginning of Section 5 and the discussion of eq. (6.7)). Measurements with finite apertures for tomographic reconstruction are also suggested by Levy and Mockett in Reference 4. In order to realize the tunnel effect estimated by Levy et al. in Reference 5 one must either know the tunnel location or register the radiation in a very wide angle of aperture. Wide aperture observations not only smear out the angular dependency but also increase the total count and the corresponding required observation times (see eq. (6.4)) over the estimates provided by Levy et al. Also, the nominal depth, that is the location of the observer in the reference plane is not very well defined if the detector extends from the ground surface to a depth of 200 m. This uncertainty possibly can reduce the accuracy of a reconstructed density distribution.

7. Conclusions.

Subterranean cosmic-ray intensity depends mainly on the average density of the material which has been penetrated by muons. Therefore, measurements of muon radiation intensity can be used to locate density anomalies in the overlaying strata. Such anomalies can represent either geological structures or man made artifacts, like tunnels. This method of locating density anomalies has been proposed in Reference 5 for the detection of tunnels, whereby the detector apparatus would be located in a bore hole. The measurements from a multitude of detectors would be combined and the density distribution above the detectors determined by tomographic reconstruction. The feasibility of this method for tunnel detection depends on the recording times which are required for the measurements. In this report, the effects of cylindrical tunnels with diameters of 2 m on the radiation intensity are calculated and the required measurement efforts estimated. The conclusion from these estimates is that the method might be feasible for tunnel detection up to detector depths of not more than 40 m. At these depths, the necessary recording times are of the order of days, approaching the order of a month in limit cases. If the depth of the detector is increased then the corresponding required recording times increase exponentially. The depths of detectable

tunnels are less than the depths of the detectors.

The average rock density was assumed to be 2700 kg/m^3 for the computation of tunnel effect estimates. Deviations from this average by some 10% are possible under normal circumstances, and they would change the depth estimates proportionally. Because of the approximate nature of the estimates, changes of this order of magnitude can be considered as negligible.

The estimates are based on simple assumptions about the properties of the radiation detector and requirements on data for a tomographic density reconstruction. It is conceivable that special data analysis methods can be developed which use prior knowledge about the tunnel (for instance, its direction and size) and are less demanding on data accuracy than a general tomographic density reconstruction. Therefore, a decision to support a construction of the proposed detector for application in tunnel detection should be based on results from a tested data interpretation program on simulated data. Such results would not only establish more accurate bounds of applicability of the method but also provide design parameters for the detector.

LIST OF REFERENCES.

1. J. C. Barton and C. T. Stockel, "Some problems in the interpretation of underground cosmic-ray data", *Canadian Journal of Physics*, 46 (1968), pp. S318-S323.
2. L. Malmquist, G. Jönsson, K. Kristiansson and L. Jacobsson, "Theoretical studies of in-situ rock density determinations using underground cosmic-ray muon intensity measurements with application in mining geophysics", *Geophysics*, 44 (1979), pp. 1549-1569.
3. Luis W. Alvarez, Jared A. Anderson, F. El Bedwei, James Burkhard, Ahmed Fakhry, Adib Girgis, Amr Goneid, Fikhry Hassan, Dennis Iverson, Gerald Lynch, Zenab Miligy, Ali Hilmy Moussa, Mohammed-Sharkawi and Lauren Yazolino, "Search for Hidden Chambers in the Pyramids", *Science*, 167 (1970), pp. 832-839.
4. Richard H. Levy and Paul M. Mockett, "Method and Apparatus for Determining the Density Characteristics of Underground Earth Formations", U.S. Patent 4504438, 1985.
5. R. H. Levy, P. Mockett and C. Tosaya, "Sensitivity Analyses of Muon Tomography for Tunnel Detection", *Third Technical Symposium On Tunnel Detection Proceedings*, Golden, Colorado, 1988, pp. 284-298.

Appendix. Comparison of Numerical Results.

We compare numerical results by Levy et al. in Reference 5 with this report to check the calculations and the adequacy of simplifying assumptions.

In our calculations, the detector diameter is 0.26 m and the detector length is 2.82 m. The dimensions of the detector are assumed to be short compared to the distance to the tunnel. The effect of the tunnel we define as the difference between observations with and without the tunnel within a solid angle corresponding to a cone with 5° half angle. A summary of the required observation effort is shown in Figure 11.

Levy et al. assume in their numerical example a detector with a diameter of 0.26 m and a length that extends from the ground surface to 200 m depth. They define the tunnel effect as the difference between observations with and without tunnel within the solid angle that is supported by the silhouette of the tunnel. A quantitative summary of their results is shown in Figure 2 of Reference 5 which displays those locations of tunnels where the effects are sufficiently large to be detected in seven days.

To compare the results one should choose comparable geometries. Therefore we select a tunnel that is close to the detector so that the 5° half angle of our aperture cone approximately corresponds to the support half angle of the tunnel cross section. The tunnel depth we choose close to 200 m so that the portion of the 200 m long detector which registers its effect, i.e. the portion that is deeper than the tunnel, is short.

Specifically, we assume $Z_0 = 190$ m and $X_0 = 5$ m, and read from Figure 2 of Reference 5 that the tunnel effect equals about $1.8 \sigma_N$ for an observation length of seven days. Because only those detector parts which are deeper than the tunnel register a tunnel effect we estimate the effective depth of the detector to about 200 m, and its effective length to about 5 m. Then the corresponding recording area is about $5 \cdot 0.26 = 1.3 \text{ m}^2$. The support half-angle of the tunnel cross section is about $\arctan(1/10)$. Levy et al. estimate that most of the tunnel effect is observed within a solid angle that is supported by the tunnel silhouette with a length twice the nearest distance to the tunnel (p. 288). The size of this solid angle which they use for their radiation estimates is

$$A_L \approx \left[2 \cdot \arctan \frac{1}{10} \right] \cdot \left[2 \cdot \arctan 1 \right] \approx 0.31 \text{ sr} . \quad (\text{A.1})$$

For $z_{\text{detector}} = 200$, $Z_0 = 190$ and $X_0 = 5$ we obtain $\Theta_0 = 26^\circ$. Figure 11 provides for this input a required observation effort of about 300 [days·m²] if the tunnel effect

should be larger than $3.16 \sigma_N$. The solid angle of the observational field is for Figure 11 assumed to be

$$A_C = 2 \pi (1 - \cos 5^\circ) = 0.024 \text{ sr} . \quad (\text{A.2})$$

Scaling our result from Figure 11 to the conditions in the Levy et al. paper we obtain for the required number of days the value

$$N \approx 300 [\text{days} \cdot \text{m}^2] \cdot \left(\frac{1.8 \sigma_N}{3.16 \sigma_N} \right)^2 \cdot \frac{0.024 [\text{sr}]}{0.31 [\text{sr}]} \cdot \frac{1}{1.3 [\text{m}^2]} \approx 6 \text{ days} \quad (\text{A.3})$$

instead of $N = 7$. The estimate (A.3) can be increased or decreased by a large factor because the estimates of the effective detector length and aperture solid angles arguably can be different and the reading of $1.8 \sigma_N$ from Figure 2 of Reference 5 is quite inaccurate. Therefore, it is easy to obtain an exact agreement between both papers. We conclude from the comparison that the results in both papers agree in order of magnitude.

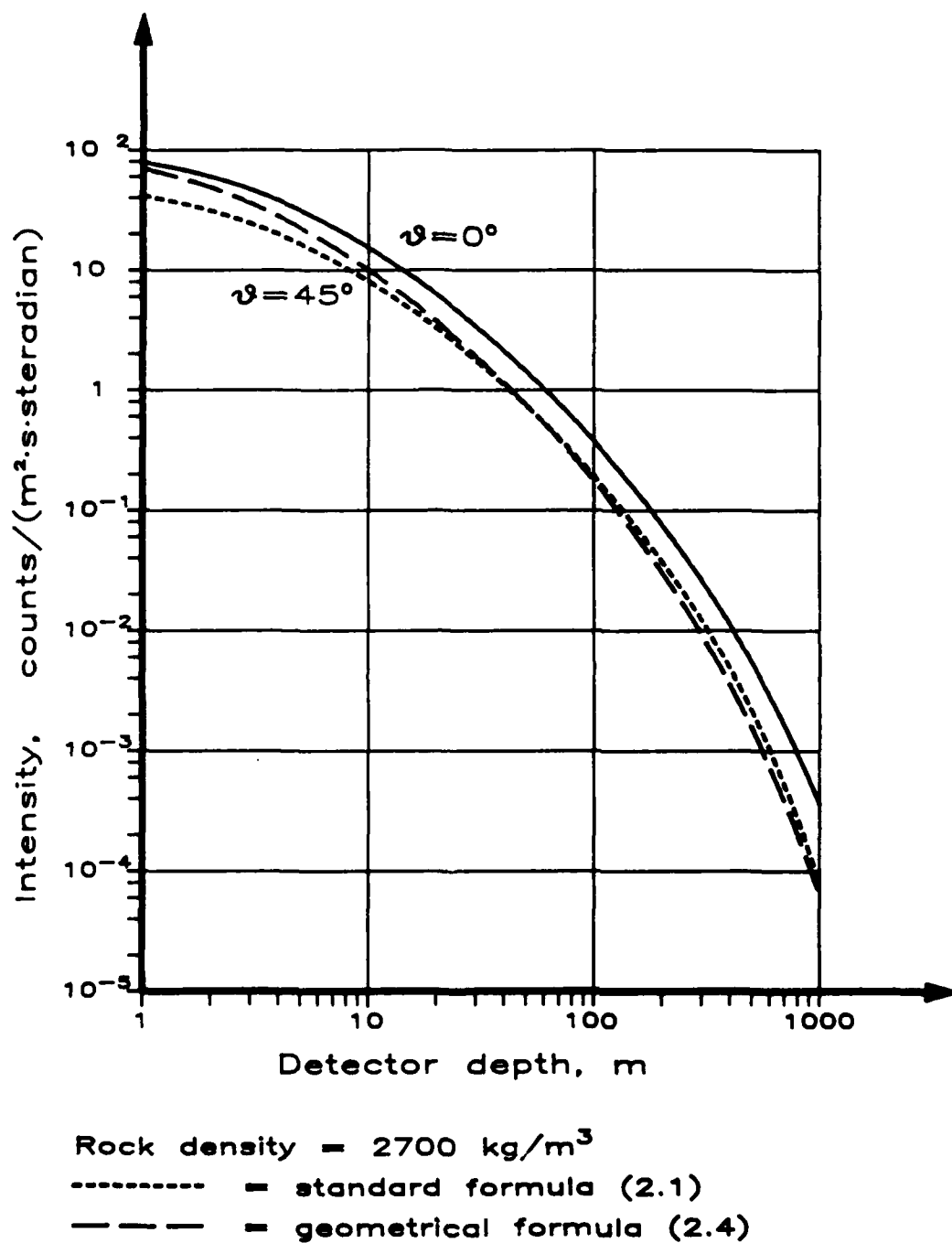


Figure 1. Normal radiation intensity.

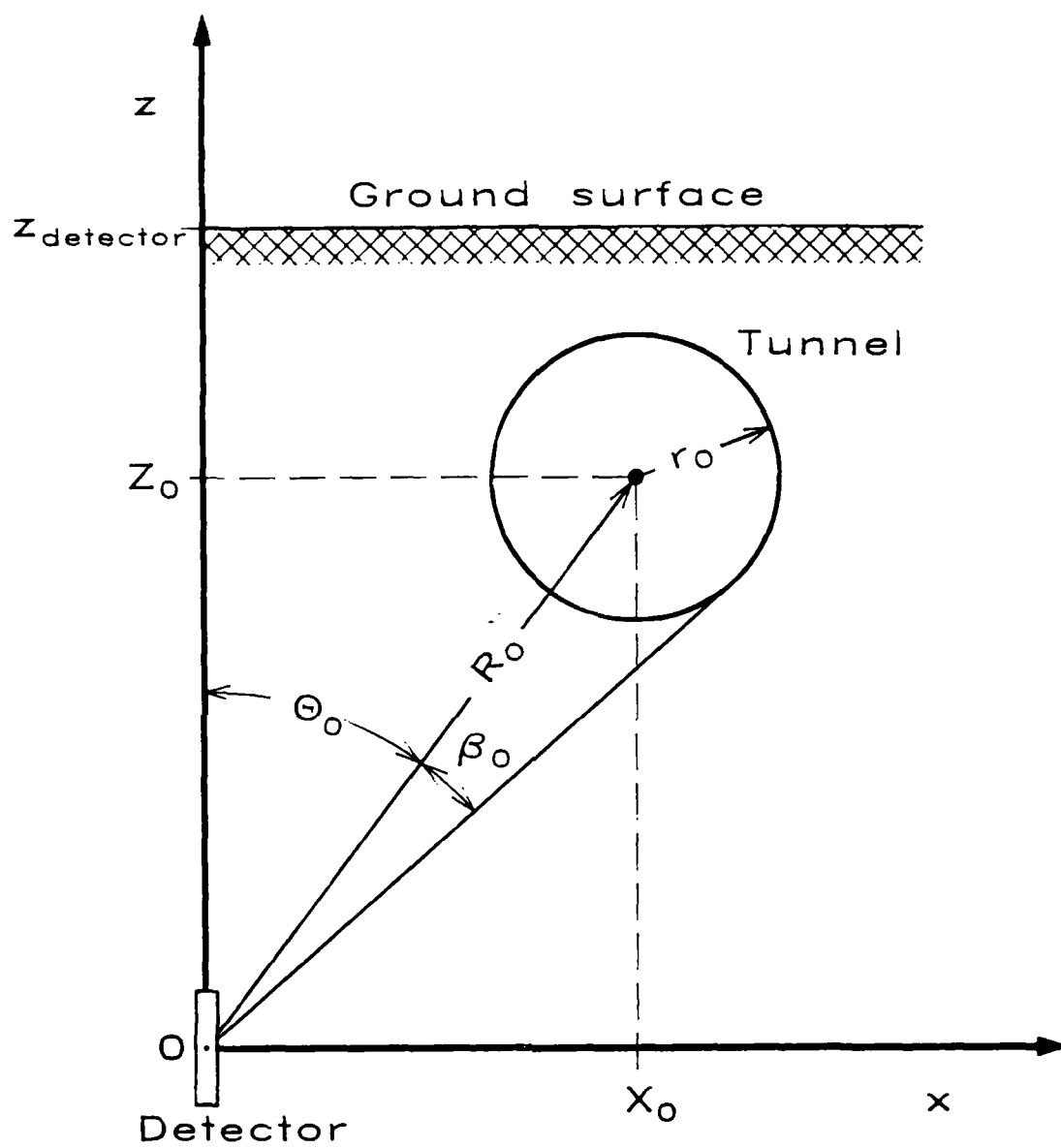


Figure 2. Tunnel coordinates.

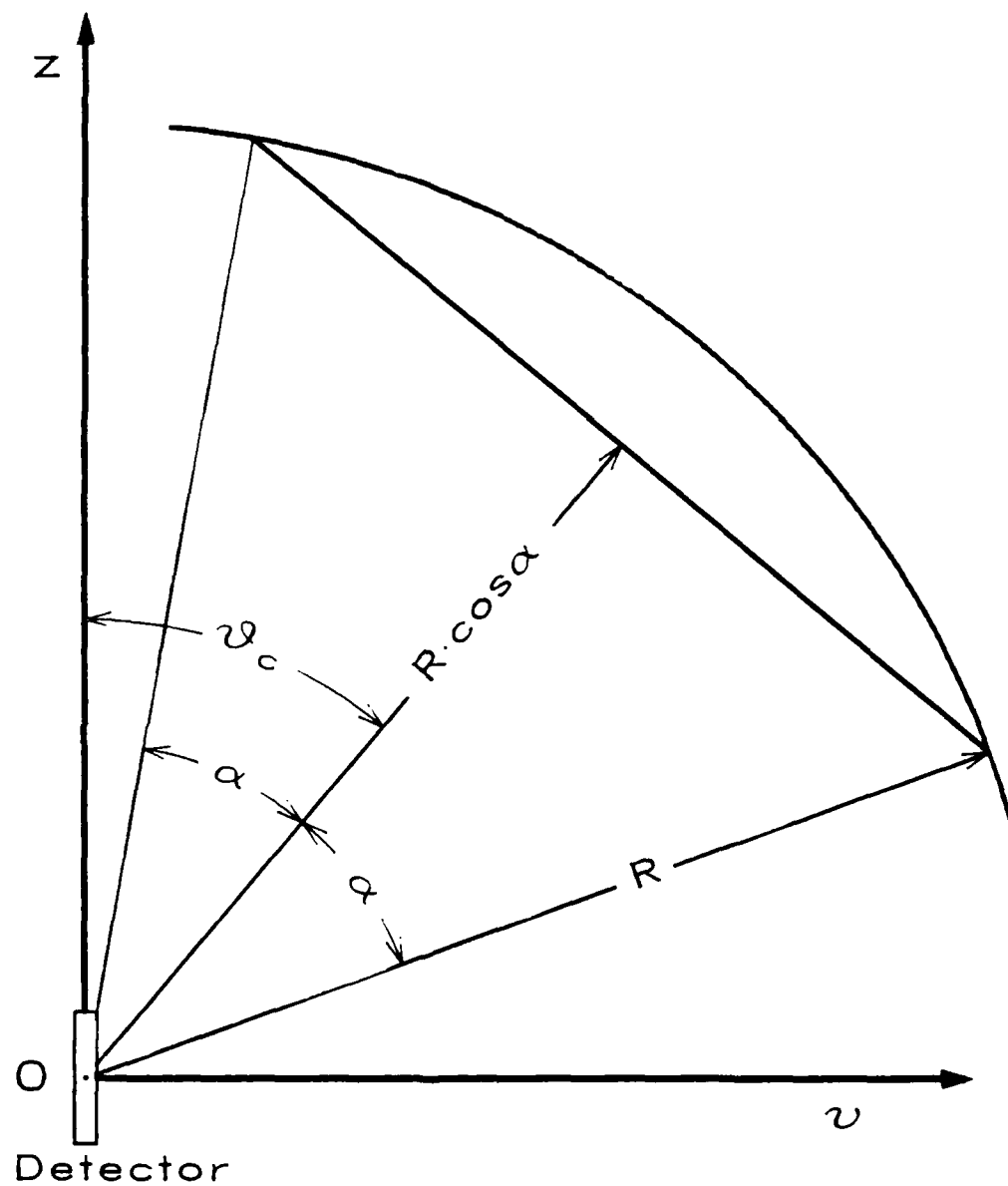
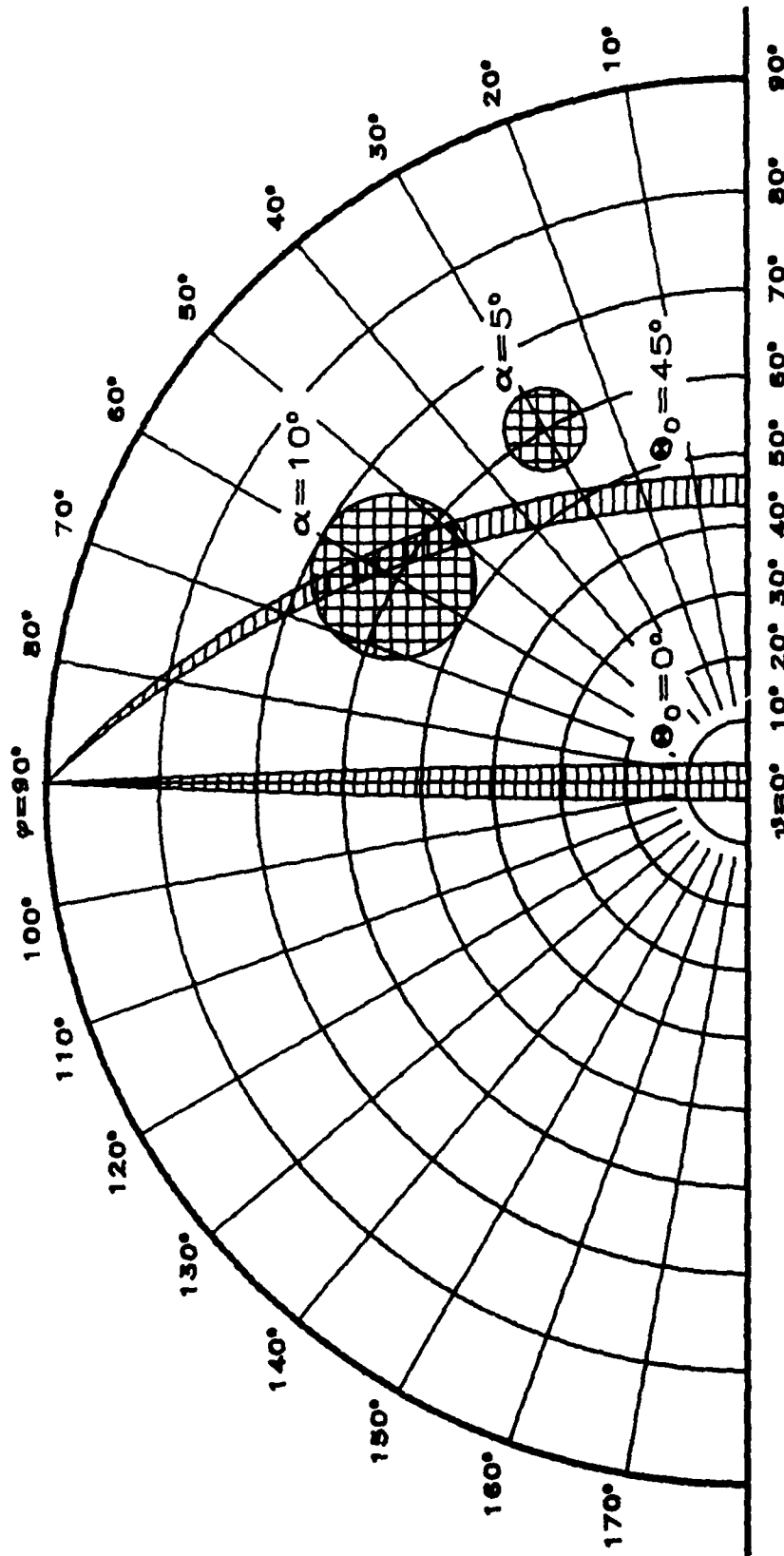
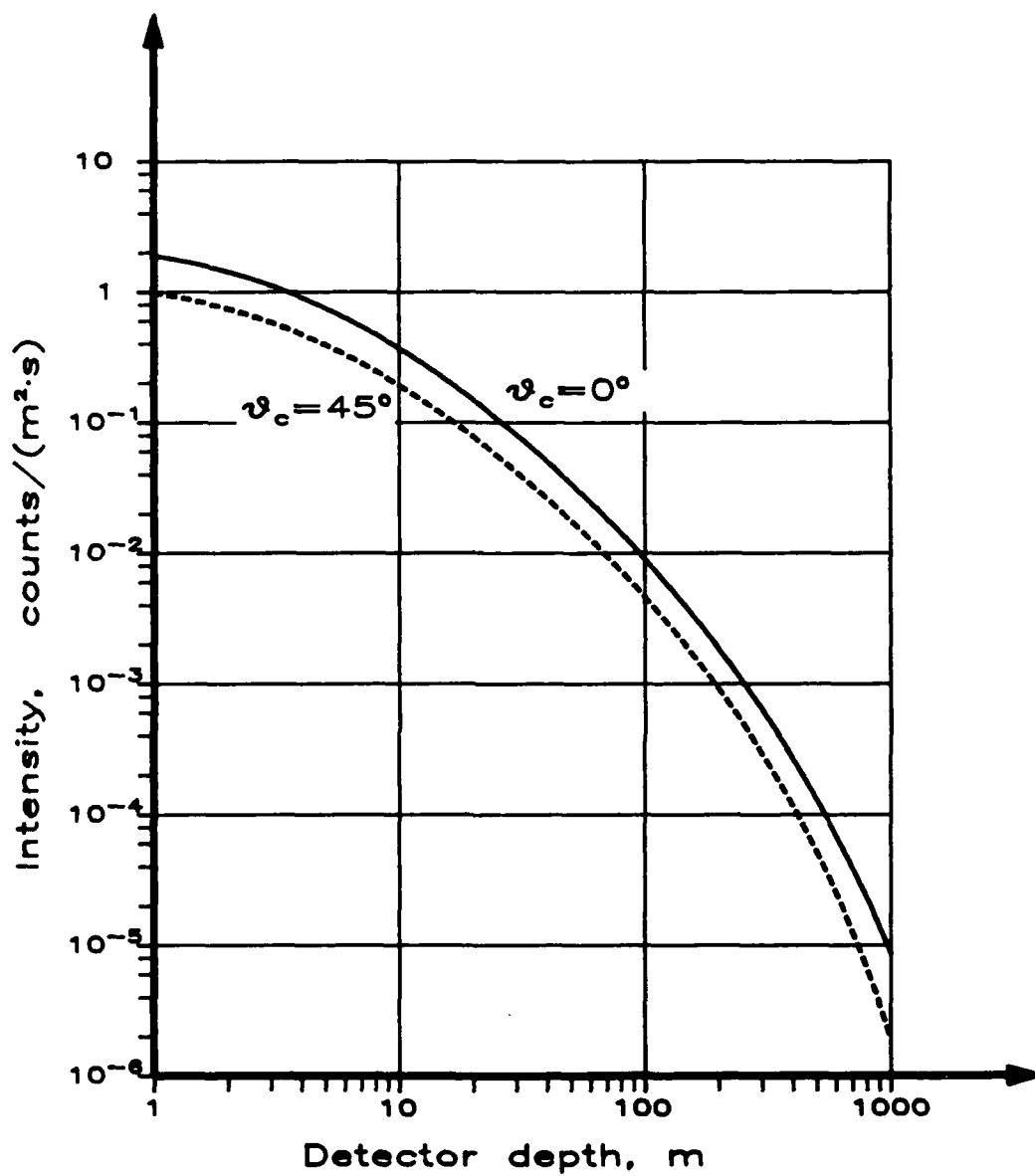


Figure 3. Aperture angle α .



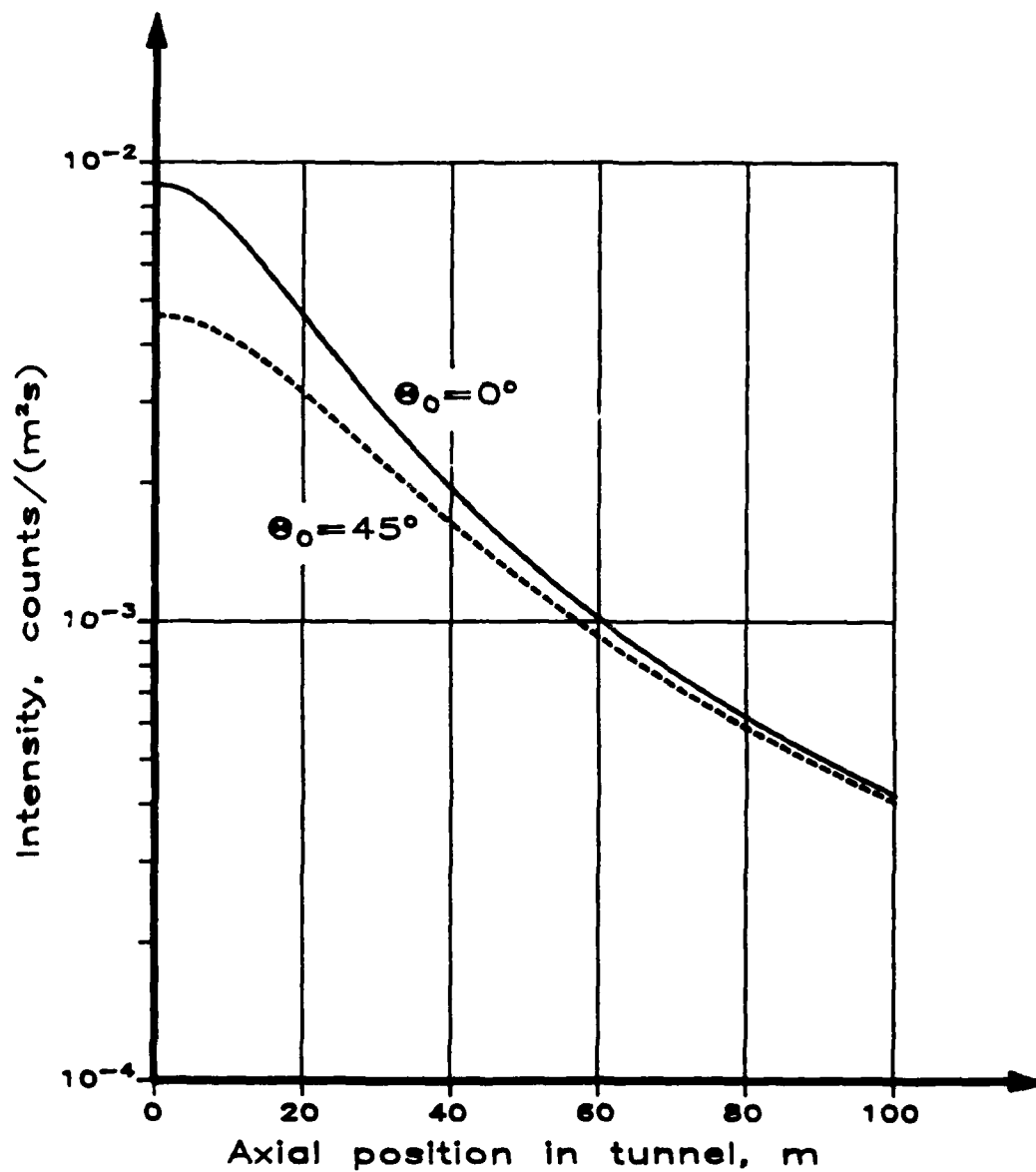
Tunnel radius $r_0 = 1.0$ m
 Vertical distance $Z_0 = 20.0$ m

Figure 4. Tunnel contours and aperture field.



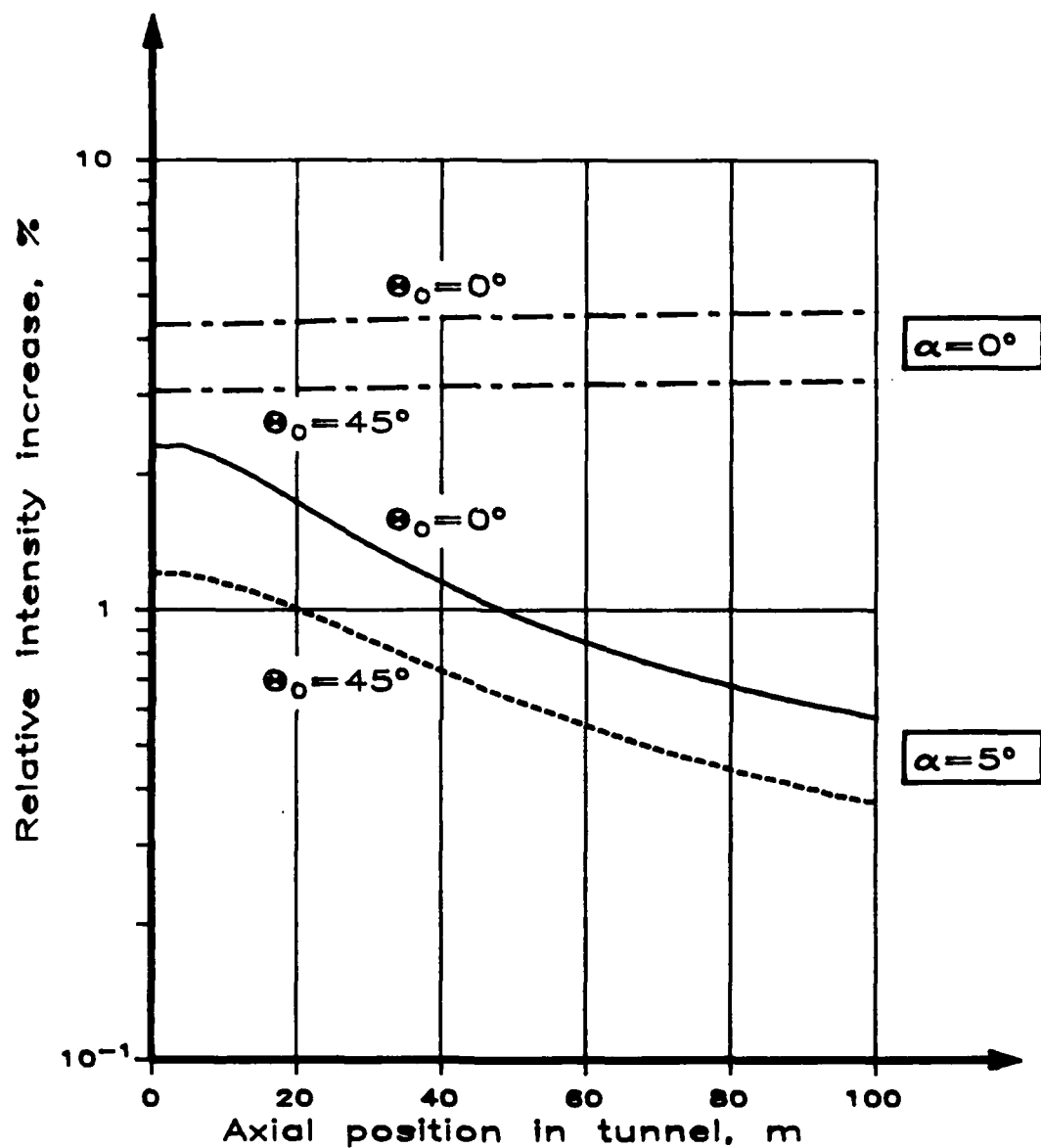
Rock density = 2700 kg/m^3
Detector aperture = 5°

Figure 5. Normal radiation intensity for a finite aperture.



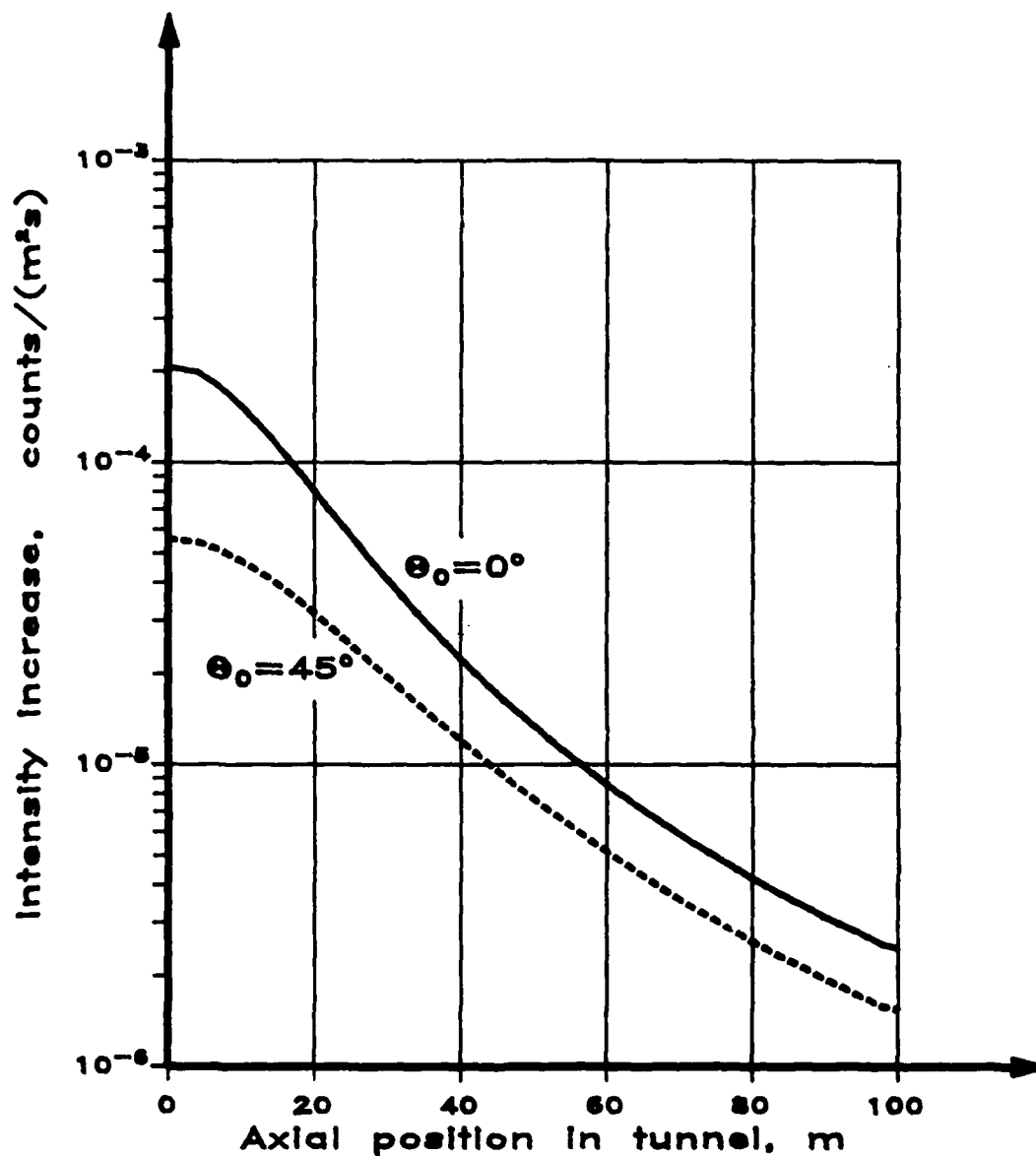
Rock density = 2700 kg/m³
 Detector depth = 100 m
 Detector aperture = 5°
 Tunnel depth = 80 m
 Tunnel radius = 1.0 m

Figure 6. Normal radiation intensity in tunnel direction.



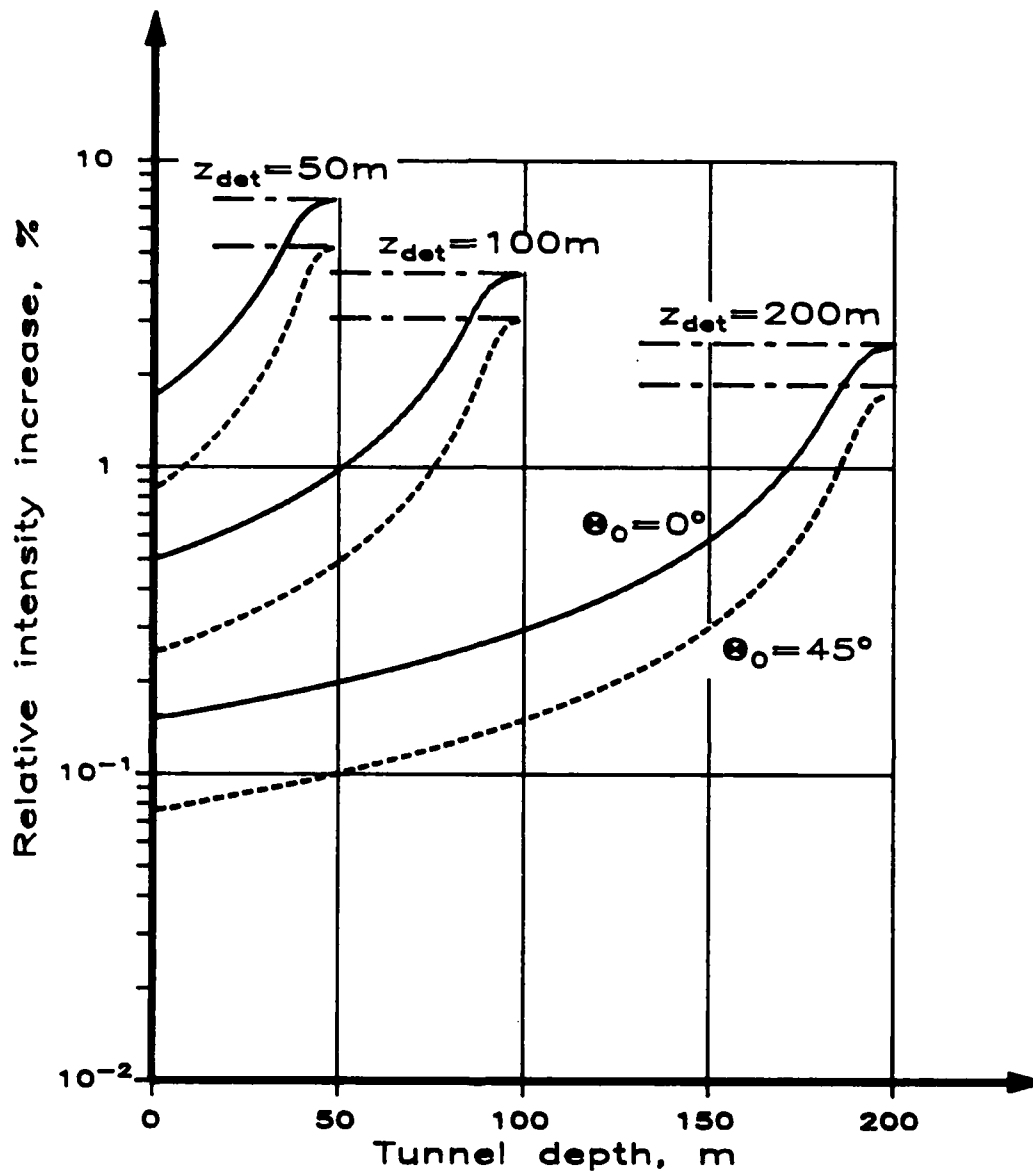
Rock density = 2700 kg/m³
 Detector depth = 100 m
 Tunnel depth = 80 m
 Tunnel radius = 1.0 m

**Figure 7. Relative tunnel effect
versus axial position.**



Rock density = 2700 kg/m³
 Detector depth = 100 m
 Detector aperture = 5°
 Tunnel depth = 80 m
 Tunnel radius = 1.0 m

Figure 8. Absolute tunnel effect versus axial position.



Rock density = 2700 kg/m³

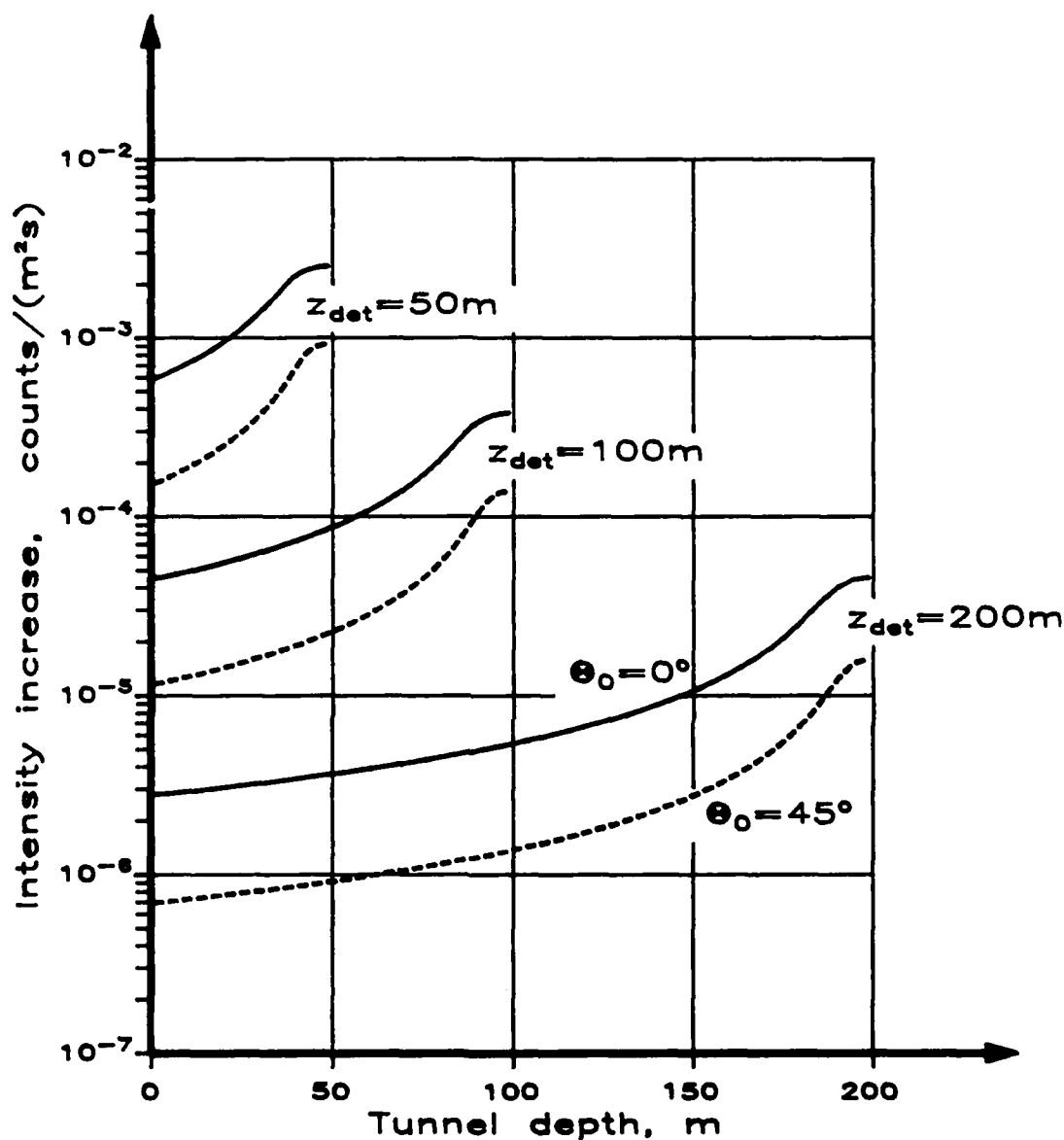
Tunnel radius = 1.0 m

----- = aperture zero

————— = aperture 5°, zenith angle zero

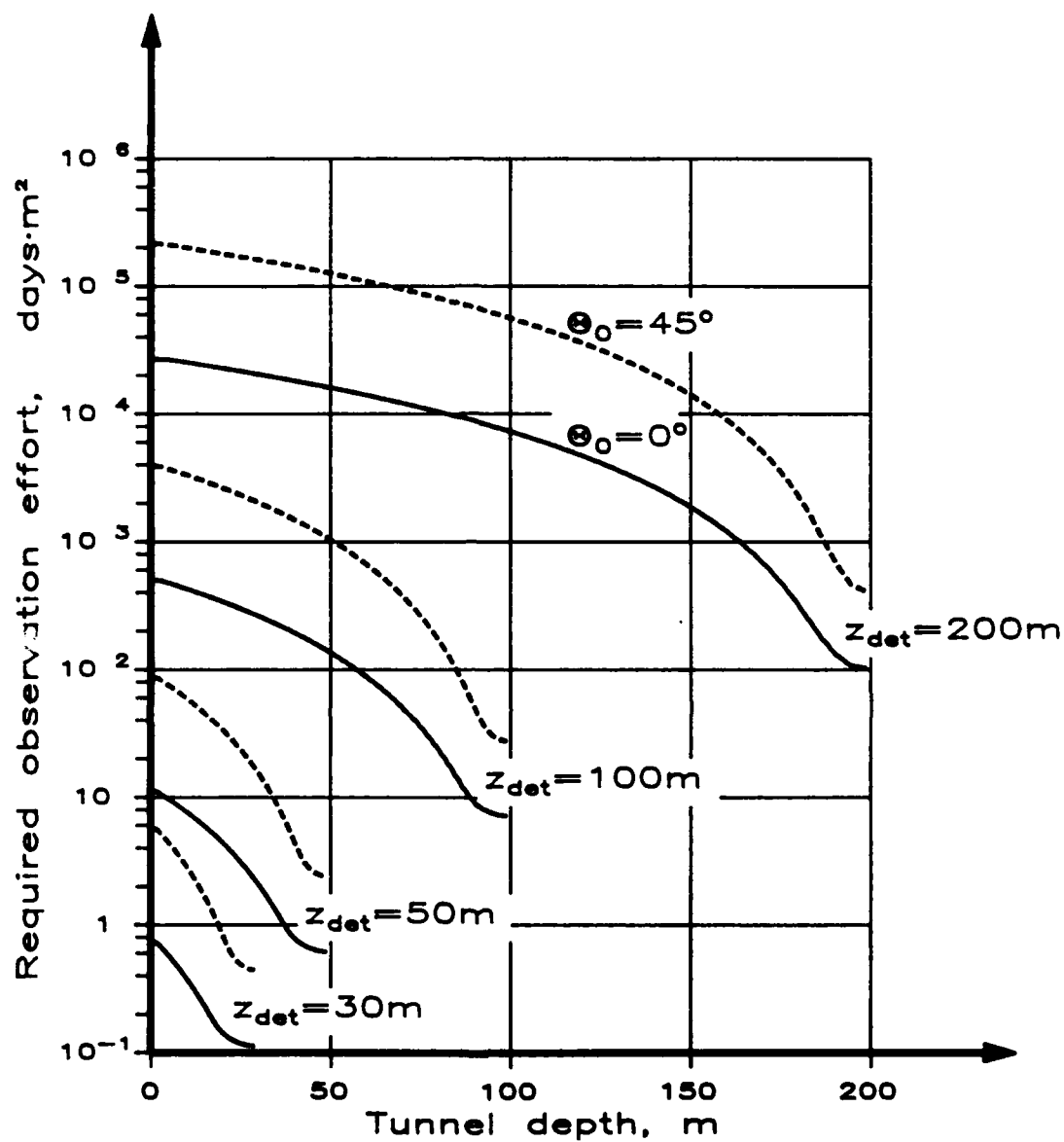
----- = aperture 5°, zenith angle 45°

**Figure 9. Relative tunnel effect
in the reference plane.**



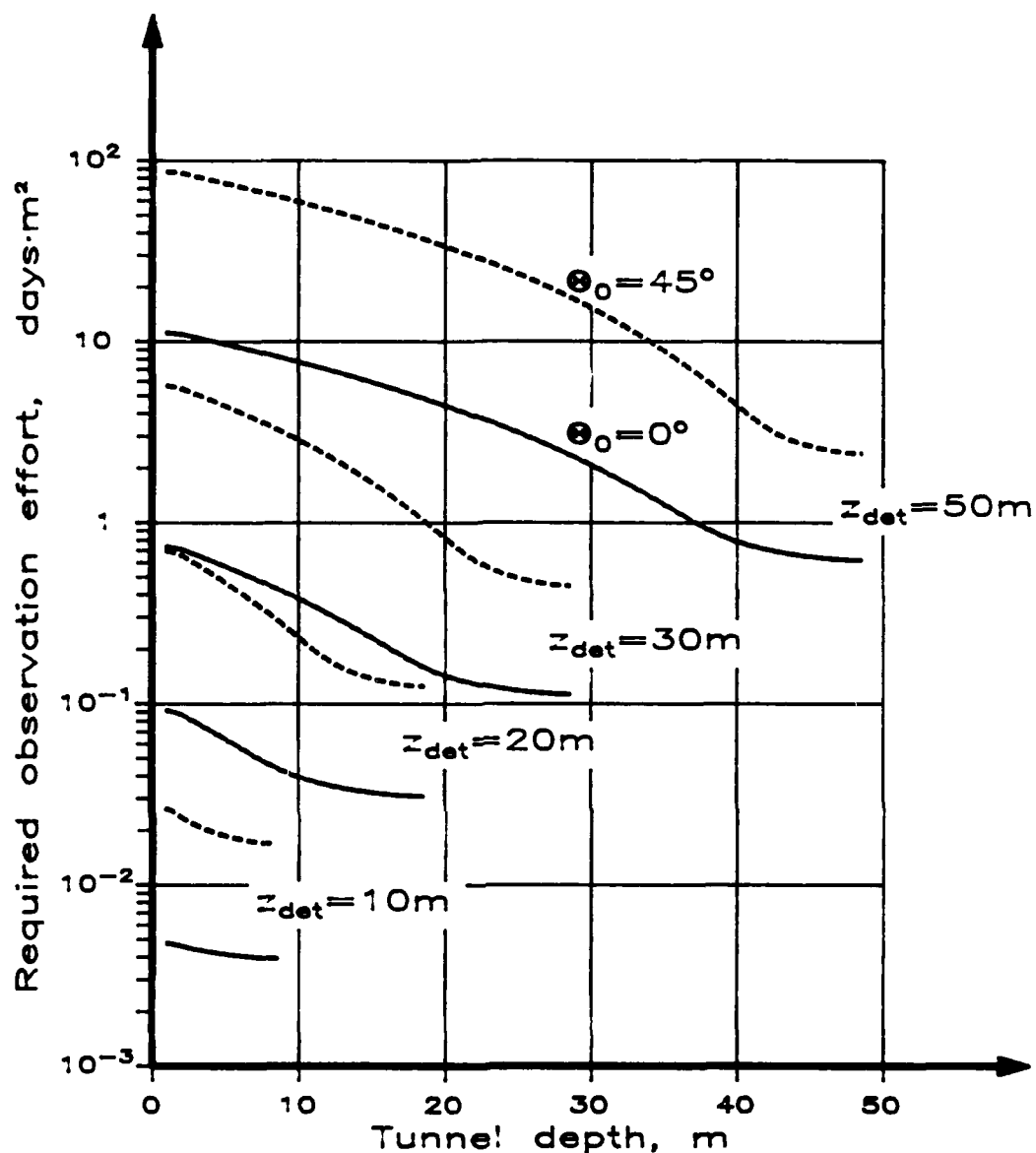
Rock density = 2700 kg/m³
 Detector aperture = 5°
 Tunnel radius = 1.0 m
 ————— = zenith angle zero
 - - - - - = zenith angle 45°

Figure 10. Absolute tunnel effect
in the reference plane.



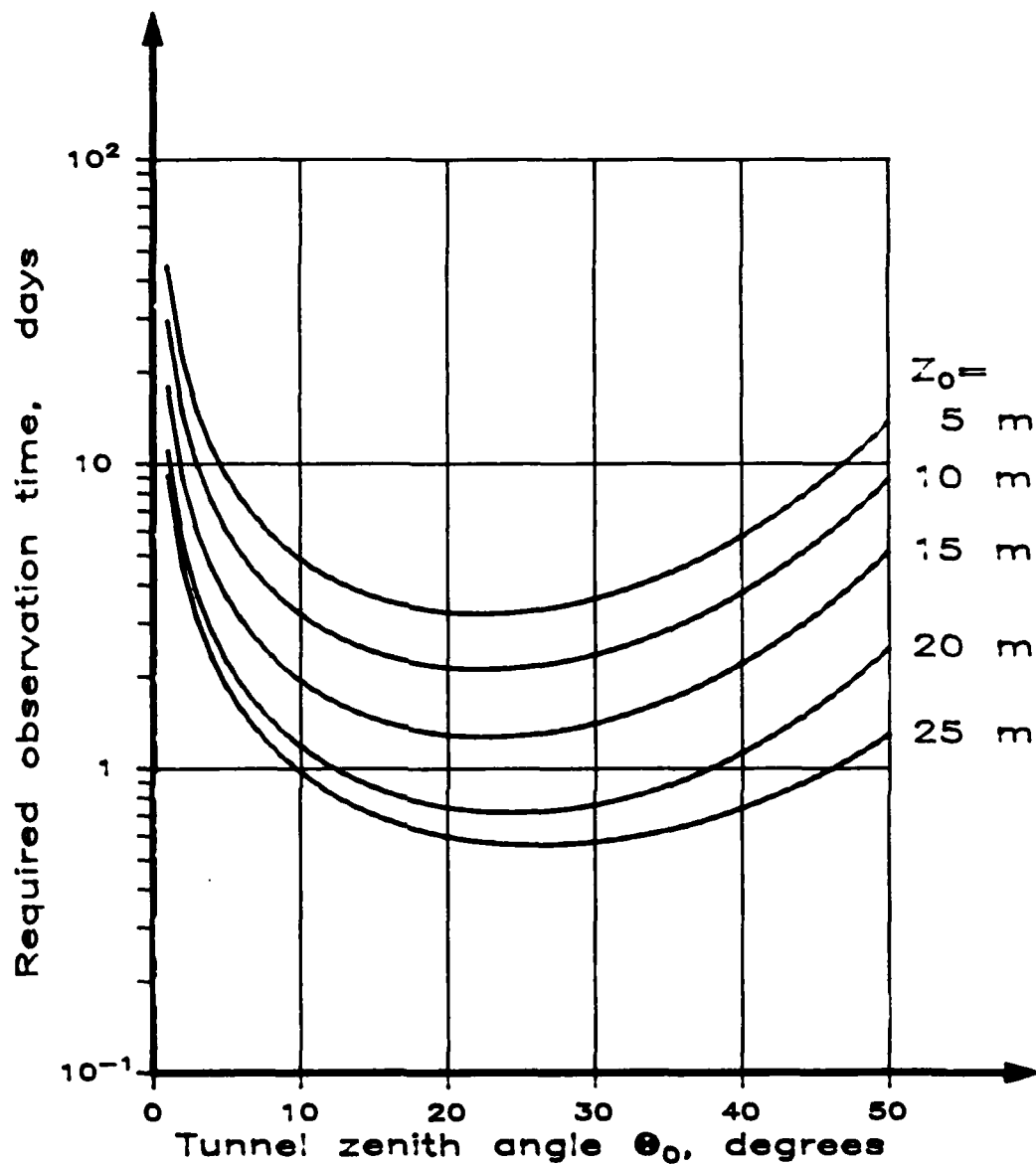
Rock density = 2700 kg/m³
 Detector aperture = 5°
 Tunnel radius = 1.0 m
 ----- = zenith angle 45°
 ————— = zenith angle zero
 Confidence factor σ/signal = 0.316

Figure 11. Required observation effort in the reference plane.



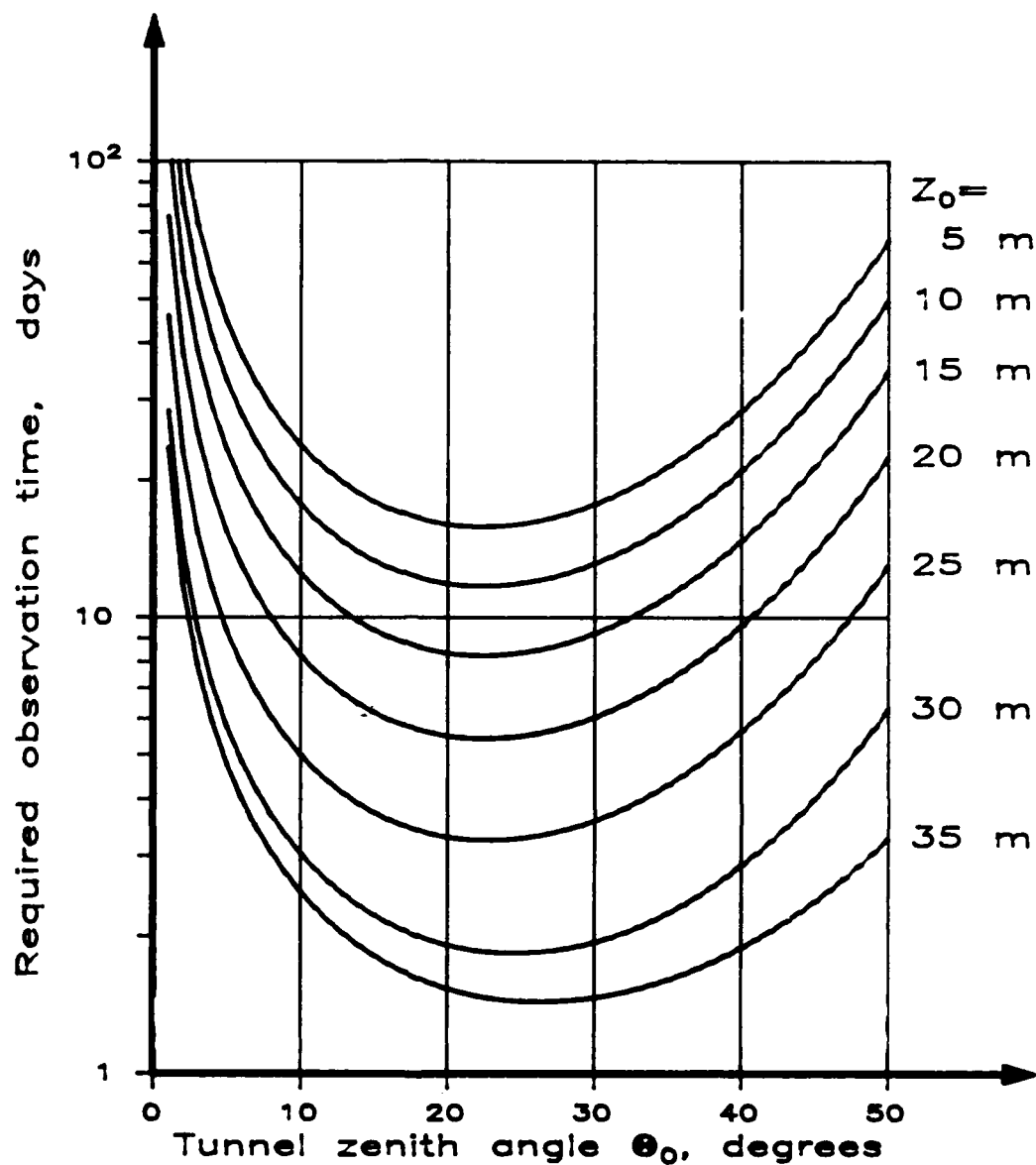
Rock density = 2700 kg/m³
 Detector aperture = 5°
 Tunnel radius = 1.0 m
 ----- = zenith angle 45°
 ————— = zenith angle zero
 Confidence factor σ_{signal} = 0.316

Figure 12. Required observation effort in the reference plane for shallow tunnels.



Rock density = 2700 kg/m³
 Detector aperture = 5°
 Detector depth = 30 m
 Tunnel radius = 1.0 m
 Confidence factor σ/signal = 0.316
 Bore hole diameter = 30 cm

Figure 13. Required observation time in the reference plane for a detector at 30 m



Rock density = 2700 kg/m^3
 Detector aperture = 5°
 Detector depth = 40 m
 Tunnel radius = 1.0 m
 Confidence factor σ/signal = 0.316
 Bore hole diameter = 30 cm

**Figure 14. Required observation time
 in the reference plane
 for a detector at 40 m**

DISTRIBUTION LIST

No of Copies	Organization	No of Copies	Organization
1	Office of the Secretary of Defense OUSD(A) Director, Live Fire Testing ATTN: James F. O'Bryon Washington, DC 20301-3110	1	Director US Army Aviation Research and Technology Activity Ames Research Center Moffett Field, CA 94035-1099
2	Administrator Defense Technical Info Center ATTN: DTIC-DDA Cameron Station Alexandria, VA 22304-6145	1	Commander US Army Missile Command ATTN: AMSMI-RD-CS-R (DOC) Redstone Arsenal, AL 35898-5010
1	HQDA (SARD-TR) WASH DC 20310-0001	1	Commander US Army Tank-Automotive Command ATTN: AMSTA-TSL (Technical Library) Warren, MI 48397-5000
1	Commander US Army Materiel Command ATTN: AMCDRA-ST 5001 Eisenhower Avenue Alexandria, VA 22333-0001	1	Director US Army TRADOC Analysis Command ATTN: ATAA-SL White Sands Missile Range, NM 88002-5500
1	Commander US Army Laboratory Command ATTN: AMSLC-DL Adelphi, MD 20783-1145	(Class. only) 1	Commandant US Army Infantry School ATTN: ATSH-CD (Security Mgr.) Fort Benning, GA 31905-5660
2	Commander US Army, ARDEC ATTN: SMCAR-IMI-I Picatinny Arsenal, NJ 07806-5000	(Unclass. only) 1	Commandant US Army Infantry School ATTN: ATSH-CD-CSO-OR Fort Benning, GA 31905-5660
2	Commander US Army, ARDEC ATTN: SMCAR-TDC Picatinny Arsenal, NJ 07806-5000	1	Air Force Armament Laboratory ATTN: AFATL/DLODL Eglin AFB, FL 32542-5000
1	Director Benet Weapons Laboratory US Army, ARDEC ATTN: SMCAR-CCB-TL Watervliet, NY 12189-4050		<u>Aberdeen Proving Ground</u>
1	Commander US Army Armament, Munitions and Chemical Command ATTN: SMCAR-ESP-L Rock Island, IL 61299-5000	2	Dir, USAMSAA ATTN: AMXSY-D AMXSY-MP, H. Cohen
1	Commander US Army Aviation Systems Command ATTN: AMSAV-DACL 4300 Goodfellow Blvd. St. Louis, MO 63120-1798	1	Cdr, USATECOM ATTN: AMSTE-TD
		3	Cdr, CRDEC, AMCCOM ATTN: SMCCR-RSP-A SMCCR-MU SMCCR-MSI
		1	Dir, VLAMO ATTN: AMSLC-VL-D

DISTRIBUTION LIST

<u>No. of</u> <u>Copies</u>	<u>Organization</u>	<u>No. of</u> <u>Copies</u>	<u>Organization</u>
1	Commander Eighth U.S. Army Tunnel Neutralization Team ATTN: LTC P. Funkhouser APO San Francisco, CA 96301	2	Southwest Research Institute ATTN: Dr. Thomas E. Owen Dr. Bob M. Duff P.O. Drawer 28510 San Antonio, TX 78284
1	U.S. Dept. of Commerce National Institute of Science & Technology ATTN: David A. Hill 325 Broadway Boulder, CO 80303-3328	1	Department of Geophysics Colorado School of Mines ATTN: Dr. Al Balch 1500 Illinois Golden, CO 80401
1	SRI International ATTN: Mr. Bob Bollen 333 Ravenswood Drive Menlo Park, CA 94025	2	Belvoir Research Development and Engineering Center ATTN: STRBE-JM (Mr. Ray Dennis) (Mr. Frank Ruskey) Fort Belvoir, VA 22060-5606
1	ENSCO ATTN: Dr. Robert Kemerait 1930 Highway A1A Indian Harbor Beach, FL 32937	1	Pennsylvania State University ATTN: Dr. Roy Greenfield State College, PA 16801
1	Associate Director for Research Kansas Geological Survey The University of Kansas ATTN: Dr. Don W. Steeples 1930 Constant Ave., Campus West Lawrence, KS 66046-2598	2	DOE/UNC Technical Services Inc. ATTN: Mr. Jim Allen Mr. Dave George P.O. Box 14000 2597 B 3/4 Road Grand Junction, CO 81502-5504
1	U.S. Department of the Interior Geological Survey ATTN: Garry R. Olhoeft P.O. Box 25046 DFC MS964 Denver, CO 80225	1	JASON MITRE ATTN: John F. Visecky P.O. Box 1474 La Jolla, CA 92038
1	Department of Geophysics and Geology University of Missouri - Rolla ATTN: Dr. Richard D. Rechten Rolla, MO 65401	1	Bechtel National, Inc. ATTN: Dr. Carol A. Josaya Fifty Beale Street P.O. Box 3965 San Francisco, CA 94119
1	Petrol Physics ATTN: Dr. Paul Mockett 2101 Third Street San Francisco, CA 94107	1	Dr. Richard H. Levy 4124 55th Avenue NE Seattle, WA 98105

DISTRIBUTION LIST

<u>No. of Copies</u>	<u>Organization</u>
1	Department of Energy Grand Junction Office ATTN: Mr. Lawrence Ball P.O. Box 2567 Grand Junction, CO 81502
1	Woodward Clyde and Associates ATTN: Dr. Walt Silva 1390 Market St., Suite 250 San Francisco, CA 94102
2	USAE Waterways Experiment Station ATTN: Dr. A. B. Franklin Mr. Robert F. Ballard, Jr. P. O. Box 631 Vicksburgh, MS 39180-0631

INTENTIONALLY LEFT BLANK.

USER EVALUATION SHEET/CHANGE OF ADDRESS

This Laboratory undertakes a continuing effort to improve the quality of the reports it publishes. Your comments/answers to the items/questions below will aid us in our efforts.

1. BRL Report Number BRL-TR-3110 Date of Report JUNE 1990
2. Date Report Received _____
3. Does this report satisfy a need? (Comment on purpose, related project, or other area of interest for which the report will be used.) _____

4. Specifically, how is the report being used? (Information source, design data, procedure, source of ideas, etc.) _____

5. Has the information in this report led to any quantitative savings as far as man-hours or dollars saved; operating costs avoided, or efficiencies achieved, etc? If so, please elaborate. _____

6. ~~General~~ Comments. What do you think should be changed to improve future reports? (Indicate changes to organization, technical content, format, etc.) _____

CURRENT
ADDRESS

Name

Organization

Address

City, State, Zip Code

7. If indicating a Change of Address or Address Correction, please provide the New or Correct Address in Block 6 above and the Old or Incorrect address below.

OLD
ADDRESS

Name

Organization

Address

City, State, Zip Code

(Remove this sheet, fold as indicated, staple or tape closed, and mail.)

FOLD HERE

DEPARTMENT OF THE ARMY

Director
U.S. Army Ballistic Research Laboratory
ATTN: SLCBR-DD-T
Aberdeen Proving Ground, MD 21005-5066
OFFICIAL BUSINESS

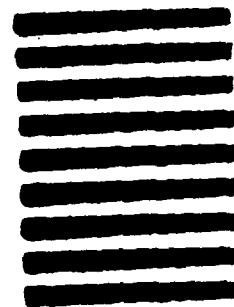


**NO POSTAGE
NECESSARY
IF MAILED
IN THE
UNITED STATES**

BUSINESS REPLY MAIL
FIRST CLASS PERMIT No 0001, APG, MD

POSTAGE WILL BE PAID BY ADDRESSEE

Director
U.S. Army Ballistic Research Laboratory
ATTN: SLCBR-DD-T
Aberdeen Proving Ground, MD 21005-9989



FOLD HERE